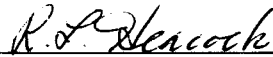


Technical Memorandum No. 33-190

***An Amplifier for Use
with Solid State Radiation Detectors
in Spacecraft Applications***

J. H. Marshall



R. L. Heacock, Chief

Lunar and Planetary Instruments

**JET PROPULSION LABORATORY
CALIFORNIA INSTITUTE OF TECHNOLOGY
PASADENA, CALIFORNIA**

October 30, 1964

Copyright © 1964
Jet Propulsion Laboratory
California Institute of Technology

Prepared Under Contract No. NAS 7-100
National Aeronautics & Space Administration

CONTENTS

I. Introduction	1
II. Basic Approach	2
III. General Theory of Operation	3
IV. Circuit Details	4
V. Stability Against Oscillation	8
VI. Gain Drifts	9
VII. Resolution	11
Table 1. Formulas for noise sources	12
References	15

FIGURES

1. Amplifier simplified schematic diagram	3
2. Amplifier schematic diagram	5
3. Amplifier transfer characteristics	6
4. Laboratory amplifier	7
5. Compensation values vs detector capacity	8
6. Conditions for oscillation	8
7. Gain correction vs detector capacity	10
8. Gain vs temperature	10
9. Distributions of noise voltage for field-effect transistors	11
10. Equivalent input noise energy	12
11. Spectra of Am^{241}	13
12. Optimum shaping time constant and resolution	14
13. Noise vs temperature	14

ABSTRACT

2648

Herein is described a charge-sensitive amplifier for use with solid state radiation detectors. Particular emphasis is placed on an analytic design approach so that optimal gain stability and resolution can be obtained for a minimum of weight and power. Measured results for an amplifier constructed for laboratory use are presented for comparison with the theoretical analysis. Presently this amplifier is being used in the second-generation Alpha Scattering Experiment on *Surveyor*.

I. INTRODUCTION

Because of their small size, rugged construction, and negligible power consumption, solid state detectors for ionizing particles have been proposed for several future interplanetary experiments. For example, the *Mariner C* Cosmic-Ray Telescope will use such detectors to measure part of the energy spectrum of interplanetary cosmic ray protons and alpha particles. Also using solid state detectors, the *Surveyor* Alpha Scattering Experiment will measure the energy of back-scattered alpha particles from the lunar surface in order to determine its composition. A similar scheme has been proposed (Ref. 1) for measuring the composition of the Martian atmosphere.

The general usefulness of these detectors prompted the development of the amplifier described below, which is intended to be part of an instrumentation system applicable to many space experiments. Several similar amplifiers already exist, but were built using a basic design approach which differs fundamentally from the one used here. After these differences are outlined, the amplifier will be described.

Future reports will contain additions to this instrumentation system as they are developed. A JPL Technical Report is presently being written describing this amplifier in more detail.

II. BASIC APPROACH

Past designs of amplifiers often resulted in gain and pulse shapes depending strongly on semiconductor parameters. The circuits were almost entirely empirically produced, because the wide variations in these parameters made accurate theoretical predictions most difficult. Since an optimum design could result only by rather improbable accident, power was wasted, and many components were present which added only to the probability of failure. Furthermore, sensistors or other temperature-variable elements were used to compensate for thermally induced semiconductor changes. This compensation, which could only be achieved by time-consuming selection of sensistors and semiconductors, resulted in poor reproducibility of circuit performance and was effective only over a very limited temperature range. Sometimes sufficiently stable operation could only be achieved by matching the drifts of one circuit to drifts of the opposite sign in a subsequent circuit. This arrangement limited the versatility of the design because circuits of the same function ceased to be interchangeable.

Virtually no provision was made for nonthermally induced semiconductor variations. The temperature-compensating schemes were particularly questionable in this regard because they required that second-order effects, such as transistor temperature coefficients, remain stable over long periods of time. The neglect of aging in circuits which had to operate for several years without repair or adjustments dangerously compromised reliability.

Finally, even with temperature compensation, experiments requiring total gain stabilities better than about 5% had to rely heavily on calibration data, providing another avenue for possible failure.

Since reliability, which obviously includes drifts not exceeding tolerance, is a prime consideration in the design of the amplifier described below, large amounts of feedback are used so that the transistor-dependent parts of the gain are of the same order as the tolerable drifts

(typically 1%). Then even large semiconductor variations perturb the gain by a tolerable amount. In addition, theoretical analysis is used to optimize the design, resulting in each circuit containing inherent stability and reliability but not using excessive weight and power. As in any carefully executed scientific approach, theoretical predictions are checked experimentally and an effort is made to understand any discrepancies present. Only when there is approximate agreement between theory and experiment can confidence be gained that a particular circuit measurement is not a special case that is difficult to reproduce.

Because temperatures are difficult to predict and control in space, the operating temperature range for this amplifier is made as large as practical, and extends from $+50$ to -50°C . The upper limit results from the intolerable noise and reduced reliability of solid state detectors operating over $+50^{\circ}\text{C}$, while the lower limit is given by the rapid decrease of transistor current gains below -50°C .

Because the variations of transistor parameters over a 100°C temperature range exceed all but the most unlikely variations caused by the aging of premium transistors over several years, stable operation during such a temperature change implies stable operation during the life of an experiment. For example, transistor current gains at -50°C are less than half their value at $+50^{\circ}\text{C}$, while the probability of a factor of 2 decrease in gain from aging is of the same order as total catastrophic failure, which hopefully is negligibly small. Obviously, if elaborate temperature compensation were provided, then the nonthermally induced drifts would be considerably greater than the thermal drifts, and this method for estimating the effect of aging would no longer be valid.

Finally, because this amplifier is sufficiently stable for most conceivable environmental conditions, calibration may be used only as an additional hedge against the unexpected, rather than as an essential part of the operation of an experiment.

III. GENERAL THEORY OF OPERATION

A simplified schematic diagram of the amplifier is shown in Fig. 1, where a capacitive current source represents the solid state detector, for which bulk resistance and leakage have been neglected. Although about 20 ns is required for most of the detector charge to be collected, the detector response is approximated by a delta-function because the collection time is short compared to the amplifier response time.

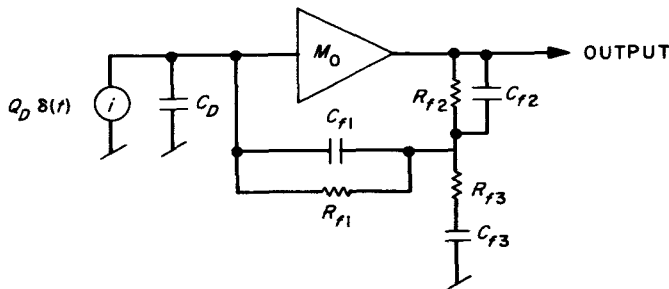


Fig. 1. Amplifier simplified schematic diagram

The charge Q_D produced by the detector is proportional to the energy loss E of a charged particle passing into the detector depletion layer and is given by

$$Q_D = q \frac{E}{E_0} \quad (1)$$

where

$$q = \text{charge on the electron} = 1.6 \times 10^{-19} \text{ C}$$

$$E_0 = \text{energy loss per hole-electron pair} = 3.5 \text{ eV in silicon}$$

The energy loss per hole-electron pair is predicted by one detector manufacturer¹ to be stable to about $\pm 1\%$ from -50 to $+50^\circ\text{C}$. So long as the particles stop within the depletion layer, the detector charge output should also be stable to about $\pm 1\%$ and independent of detector bias voltage. Because the detector capacity C_D depends on the bias voltage, which may not be particularly stable, the amplifier is designed to have an effective input capacity much larger than the detector capacity. Then most of the detector charge is deposited on the feedback capacitor C_{f1} , and the output voltage becomes nearly independent of the detector capacity and of transistor parameters, making this circuit truly a charge-sensitive amplifier.

A conversion gain of 1 V/MeV was chosen for this amplifier so that the output signal levels are high enough to avoid the need for a subsequent amplifier with its attendant weight, power, and drifts. In order to achieve this gain with a practical value of capacitance (5 pF) and in order to provide a convenient place for pulse shaping, an attenuator (Z_{f2} and Z_{f3}) is placed between the feedback capacitor and the output. The output voltage is then approximately related to the particle energy loss by

$$\frac{V_{out}}{E} \simeq \frac{q}{E_0 C_{f1}} \left(\frac{Z_{f2}}{Z_{f3}} \right) = \frac{q R_{f2}}{E_0 C_{f1} R_{f3}} \frac{p \tau_{f3}}{(1 + p \tau_{f2})(1 + p \tau_{f3})} \quad (2)$$

where

$$\tau_{f2} = \text{rise time constant} = R_{f2} C_{f2}$$

$$\tau_{f3} = \text{decay time constant} = R_{f3} C_{f3}$$

$$p = \text{Laplace transform variable}$$

$$Z_{f3} \ll Z_{f2} \quad M_0 \rightarrow \infty$$

$$Z_{f3} \ll Z_{f1} \quad R_{f1} \rightarrow \infty$$

In order to obtain the optimum signal-to-noise ratio (Ref. 2) and a pulse slowly varying near the peak, the rise time constant is made equal to the decay time constant, and the output voltage as a function of time is approximately

$$\frac{V_{out}}{E} = e M_c \left(\frac{t}{\tau} \right) \exp - \left(\frac{t}{\tau} \right) \quad (3)$$

where

$$\tau = \text{shaping time constant} = \tau_{f2} = \tau_{f3}$$

$$M_c = \text{conversion gain} = \frac{\text{pulse peak voltage}}{\text{particle energy loss}}$$

$$M_c = \frac{q R_{f2}}{e E_0 C_{f1} R_{f3}}$$

$$e = 2.72 = \text{base of natural logarithms}$$

Because the pulse shaping is done within the amplifier rather than later, no additional amplifier dynamic range is required as a result of the pulse shaping, although equal rise and fall time constants reduce the conversion gain by a factor of $1/e$.

¹Solid State Radiations, Inc., Los Angeles, Calif.

The value for the shaping time constant is a compromise between maximum tolerable counting rates, noise, and amplifier bandwidth, and can be varied to suit a particular experiment. The amplifier described in detail here used a $2\text{-}\mu\text{s}$ shaping time constant. A version with a $0.5\text{-}\mu\text{s}$ shaping time constant and a conversion gain of 0.5 V/MeV was also found to operate satisfactorily, although final optimization on such a circuit has not been performed.

Finite R_{f1} causes a 15% undershoot of the pulse for $\tau = 2\text{ }\mu\text{s}$ and $R_{f1}C_{f1} = 25\text{ }\mu\text{s}$. The area of this undershoot equals the area of the positive part of the pulse because detector current does not flow continuously. Therefore, for linear circuits, no net charge is transferred to any coupling capacitors. The baseline will have recovered to 0.25% of the pulse peak voltage after $100\text{ }\mu\text{s}$, permitting counting rates as high as 10 kc with less than 1% pile-up of the pulse tails.

IV. CIRCUIT DETAILS

Because the amplifier open-loop gain and bandwidth are finite, some charge flows onto the detector capacity and onto the amplifier input capacity. Because this charge loss depends upon unstable transistor parameters and detector capacity, the amplifier gain and bandwidth must be made as large as possible without resorting to complex circuits or to large power consumption. Two versions of the basic amplifier configuration (Fig. 2) were developed. One is intended for spacecraft applications; the other is for ground based laboratory use. The latter compromises reliability for ease in selecting components and for versatility in operating with any detector capacity without circuit changes. In the spacecraft version, the amplifier is optimized to the capacity of the detector with which it is being operated, and the transistors are stringently selected to provide a large allowance for deterioration caused by aging.

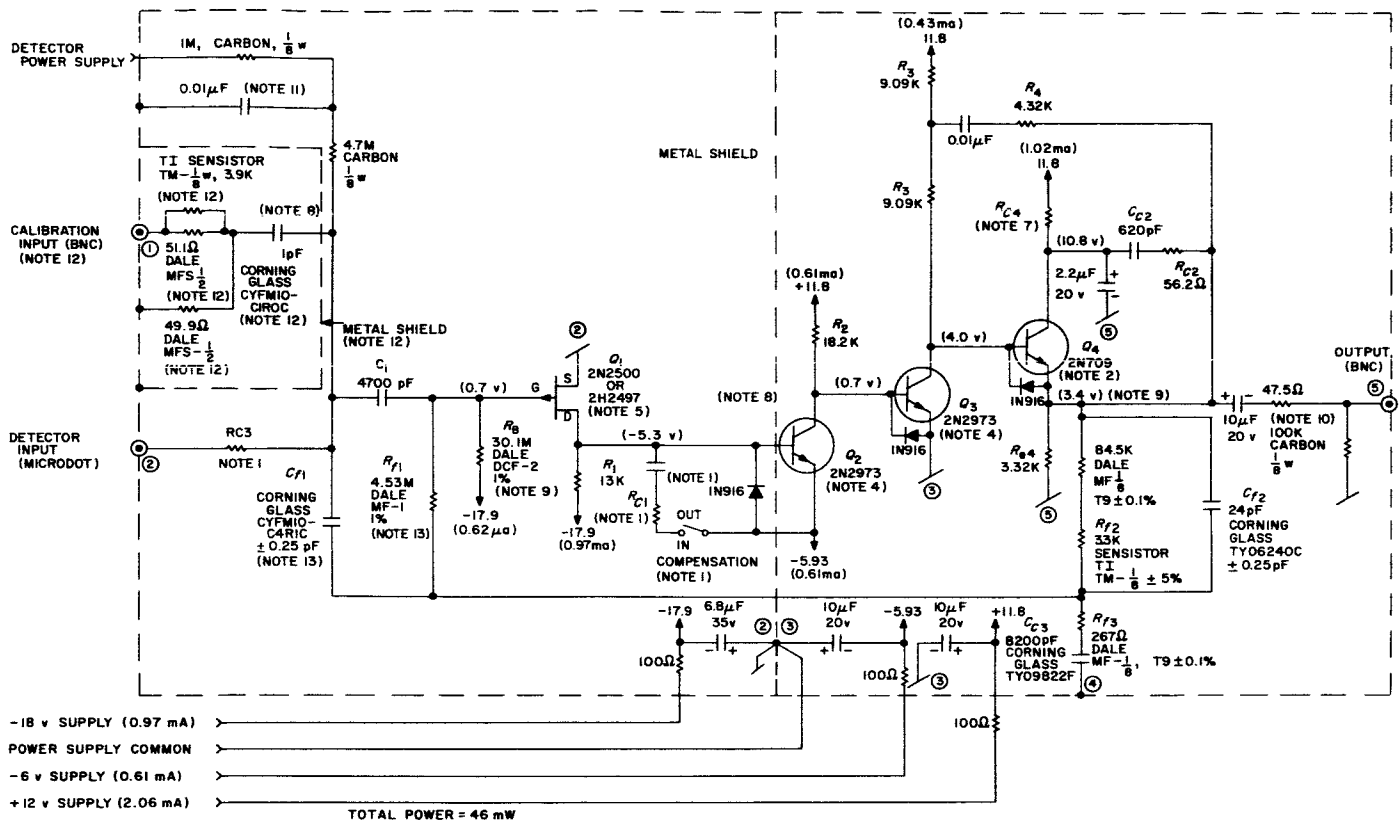
The basic configuration consists of a grounded source field-effect transistor input stage, two grounded-emitter stages, and an emitter follower output stage. Negative feedback with pulse shaping as described in the previous section is applied from the output back to the input. In order to make the dc gate voltage of the input transistor independent of the detector bias voltage, the detector is capacitively coupled to the amplifier. The size of this capacitor (C_1) can be reduced a factor of 10 without increasing the drifts if the feedback capacitor is returned directly to the detector instead of to the gate of the field-effect transistor. A small capacitor reduces the physical

size of the amplifier and decreases the sensitivity to low-frequency detector noise.

A field-effect transistor was chosen for the input stage (Q_1) because of its low noise and high input impedance. Because the noise of a field-effect transistor is nearly independent of its standing current, the transistor can be operated with a sufficiently large drain current to produce a transconductance over $1500\text{ }\mu\text{mho}$. The gate current, which is usually much smaller than detector leakage current, adds negligibly to the noise and to bias instabilities even at high impedance levels. The added complexity of the usual cascode configuration for the input stage was found not to be justified by reduced noise.

The 2N2497 or 2N2500 field-effect transistors were chosen because of their low noise figure, high transconductance, and small capacity. Also, they would operate safely at the 1 mA of drain current required for obtaining optimum gain and bandwidth.

Most of the voltage gain is provided by the second and third stages (Q_2 and Q_3), both of which are in the same TO-18 can. Because of the large voltage gain, the bandwidth is determined primarily by the collector-base capacity. The principal advantages of the 2N2973 transistors are their high current gain (typically 450) and their low collector-base capacity (3.3 pF). For the spacecraft version, the transistors are selected to have current gains that equal or exceed the typical value.



NOTES FOR LABORATORY VERSION

1. $R_1 = 56.2 \Omega$, $R_3 = 100 \Omega$, AND $C_1 = 200 \text{ pF}$. COMPENSATION MUST BE IN FOR DETECTOR CAPACITY LESS THAN 50 pF .
2. SELECT FOR $I_e \geq 1.5 \text{ mA}$ AT $I_b = 0.02 \text{ mA}$, $V_{ce} = 5 \text{ V}$ ($\beta \geq 75$). TO-18 CAN.
3. ALL RESISTORS IRC RN60C, UNLESS OTHERWISE NOTED. ALL CAPACITORS LESS THAN 1000 pF ELMENCO SILVER MICA, TEMPERATURE CHARACTERISTIC E, UNLESS OTHERWISE NOTED.
4. SELECT FOR $I_e \geq 0.6 \text{ mA}$ AT $I_b = 0.002 \text{ mA}$, $V_{ce} = 5 \text{ V}$ ($\beta \geq 300$). Q_2 AND Q_3 ARE IN THE SAME TO-18 CAN, WHICH SHOULD BE GROUNDED NEAR THE EMITTER OF Q_1 .
5. SELECT FOR $I_{sc} \geq 1.5 \text{ mA}$ AT $V_{ce} = 0$, $V_{eb} = -5 \text{ V}$, $G_m \geq 1500$ AT $I_{sc} = 1.0 \text{ mA}$, $V_{eb} = -5 \text{ V}$. LOW NOISE UNIT (SEE SECTION VII) TO-5 CAN.
6. CIRCLED NUMBERS REFER TO COMMON GROUND POINTS.
7. $R_{e1} = 1.0 \text{ K}$.
8. KEEP INDICATED LEADS AS SHORT AS POSSIBLE.
9. MATCH R_e TO Q , SO THAT THE EMITTER OF Q IS AT 3.4 V .
10. USE VALUES SHOWN FOR GENERAL-PURPOSE OPERATION.
11. $0.15 \mu\text{F}$ —100 VDC, SPRAGUE CP 08A1K8154K CAPACITOR MAY BE USED TO FILTER 60-CPS RIPPLE ON DETECTOR POWER SUPPLY.
12. OMIT THESE COMPONENTS IF THE CALIBRATION INPUT IS NOT REQUIRED.
13. MATCH C_1 TO THE CAPACITY ACROSS R_1 , SO THAT THE TOTAL CAPACITY IS $5.1 \text{ pF} \pm 1\%$.

NOTES FOR SPACECRAFT VERSION

1. SEE FIG. 9 FOR VALUES OF R_{e1} , R_{e2} , AND C_1 , AS A FUNCTION OF DETECTOR CAPACITY. OMIT SWITCH.
2. SELECT FOR $I_e \geq 2.0 \text{ mA}$ AT $I_b = 0.02 \text{ mA}$, $V_{ce} = 5 \text{ V}$ ($\beta \geq 100$). TO-18 CAN.
3. ALL RESISTORS IRC RN60C, UNLESS OTHERWISE NOTED. ALL CAPACITORS LESS THAN 1000 pF ELMENCO SILVER MICA, TEMPERATURE CHARACTERISTIC E, UNLESS OTHERWISE NOTED.
4. SELECT FOR $I_e \geq 0.8 \text{ mA}$ AT $I_b = 0.002 \text{ mA}$, $V_{ce} = 5 \text{ V}$ ($\beta \geq 400$). Q_2 AND Q_3 ARE IN THE SAME TO-18 CAN, WHICH SHOULD BE GROUNDED NEAR THE EMITTER OF Q_1 .
5. SELECT FOR $I_{sc} \geq 2.0 \text{ mA}$ AT $V_{ce} = 0$, $V_{eb} = -5 \text{ V}$, $G_m \geq 1500$ AT $I_{sc} = 1.0 \text{ mA}$, $V_{eb} = -5 \text{ V}$. LOW NOISE UNIT (SEE SECTION VII) TO-5 CAN.
6. CIRCLED NUMBERS REFER TO COMMON GROUND POINTS.
7. ADJUST TO DESIRED DYNAMIC RANGE ACCORDING TO EQ. (6). $R_{e1} \geq 1.0 \text{ K}$.
8. KEEP INDICATED LEADS AS SHORT AS POSSIBLE.
9. MATCH R_e TO Q , SO THAT THE EMITTER OF Q IS AT 3.4 V .
10. OMIT $10 \mu\text{F}$, 46.7Ω , AND 100 K . CONNECT OUTPUT DIRECTLY TO CIRCUITS WITH CAPACITIVELY COUPLED INPUTS. CAPACITIVELY COUPLE TO 200- μs TIME CONSTANT TO CIRCUITS WITH DC COUPLED INPUTS.
11. $0.01 \mu\text{F}$ SHOULD BE SUFFICIENT FOR MOST APPLICATIONS.
12. OMIT THESE COMPONENTS IF THE CALIBRATION INPUT IS NOT REQUIRED.
13. MATCH C_1 TO THE CAPACITY ACROSS R_1 , SO THAT THE TOTAL CAPACITY IS $5.1 \text{ pF} \pm 1\%$.

Fig. 2. Amplifier schematic diagram

An emitter-follower output stage (Q_4) provides a low output impedance, so that difficulties with nonlinearities and gain drifts associated with a separate buffer outside the feedback loop are minimized without large standing currents. The transistor for this stage must have a high gain-bandwidth product so as to prevent ringing for capacitive loads, and also a sufficiently large current gain to produce a low output resistance. For the spacecraft amplifier, this transistor is selected to have a current gain

in excess of 100 so that loads as small as 1 K do not appreciably increase the drifts.

In order to increase the voltage gain of the third stage without increasing power consumption, the load resistor for the third stage is boot-strapped to the emitter-follower output. This configuration also provides nearly constant base drive to the output stage, resulting in improved linearity and decreasing the problem with rate limiting

caused by the capacity on the collector of Q_3 . The resistor values are chosen so that the effective resistance of the 9.01K resistor is increased to 36.4K.

The transistor operating points are fixed by the same feedback loop which determines the ac gain, reducing complexity by eliminating coupling and bypass capacitors. The choice of operating points is a compromise between gain, bandwidth, load dependence, noise, and power consumption. Fast response and small load dependence require currents to be as large as possible, while low noise, low power consumption, and field-effect transistor limitations require small currents. The values shown in Fig. 2 represent a compromise between these conflicting requirements.

The maximum output voltage is determined by the point at which Q_4 saturates. If the field-effect transi-

tor leakage current is neglected, the maximum output voltage is

$$V_{max} = 11.8 \text{ V} - \left[\frac{R_{c4} + R_{e4}}{R_{e4}} \right] \left[V_{gs} + \frac{V_{gs} + 17.9 \text{ V}}{R_B} R_{f1} \right] - V_{sat} \quad (4)$$

where

V_{gs} = gate-source voltage of Q_1

V_{sat} = saturation voltage of $Q_4 \simeq 0.2 \text{ V}$ to 0.5 V for load resistances between infinity and 1K.

If the power supply voltages remain constant, the principal sources of drift in V_{max} are variations in R_B and V_{gs} . Although V_{gs} may vary as much as 0.5 V between different transistors, it remains stable to about 0.1 V over the

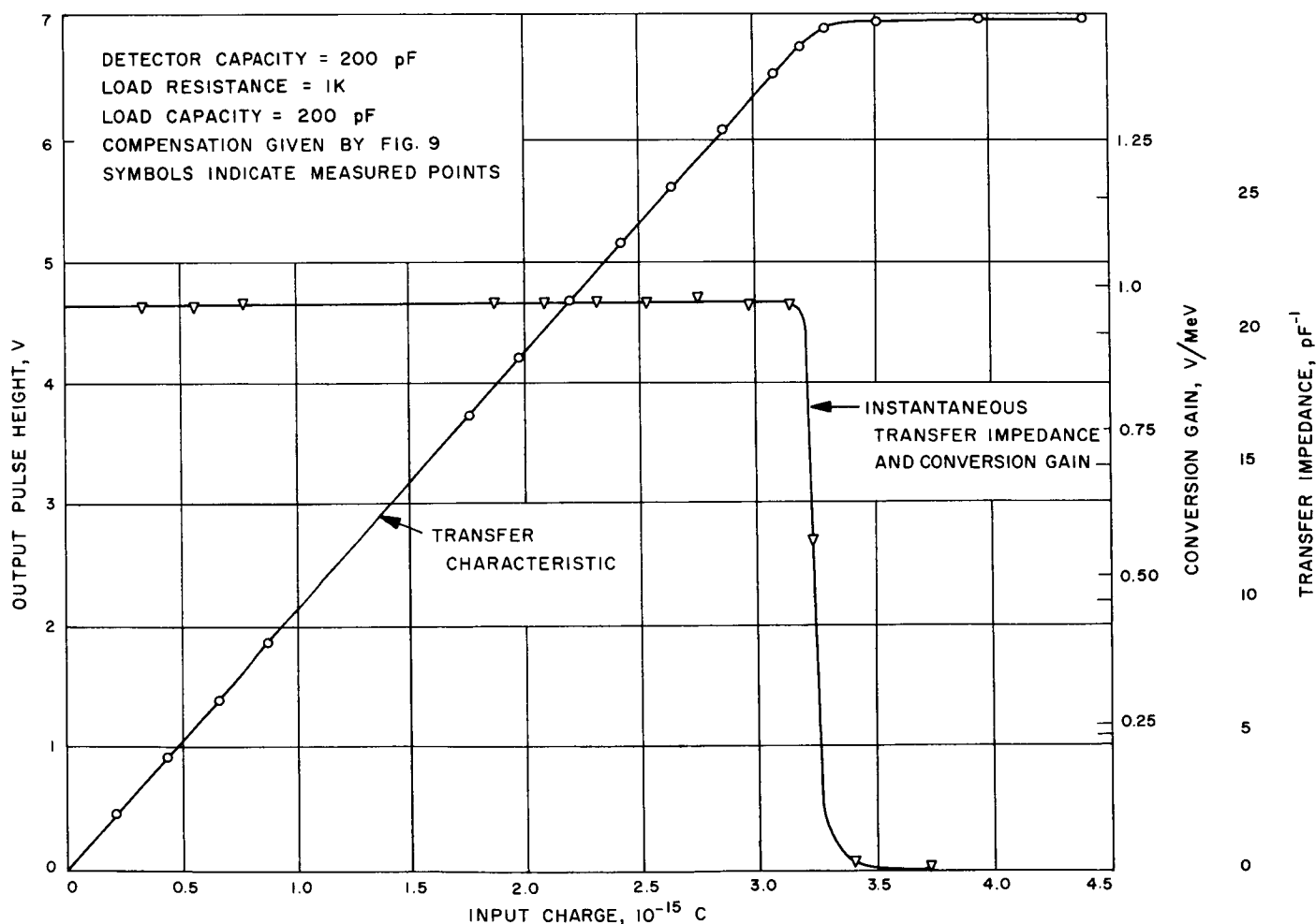


Fig. 3. Amplifier transfer characteristics

temperature range. For critical applications R_B is matched to the particular field-effect transistor being used, so that the voltage on the emitter of Q_1 equals its optimum value of 3.4 V. If R_B were a composition carbon resistor, which may have a temperature coefficient as large as 1500 ppM/°C, the maximum output voltage could drift from this cause alone by ± 0.4 V. In applications where stability of the amplifier dynamic range is important, a carbon film resistor, which is physically large but has a temperature coefficient less than 500 ppM/°C, reduces this drift to ± 0.1 V. Experimentally, the maximum output voltage is found to remain stable to 0.15 V for temperatures between -50 and $+50^\circ\text{C}$.

The maximum output voltage is limited by the available supply voltage and by the current gain and collector breakdown voltage of Q_1 . For spacecraft applications, the maximum output voltage should not exceed 5 V for 1K loads or 7 V for 2K or higher loads. As shown by Eq. (4), the dynamic range can be reduced by increasing R_{c1} .

The laboratory amplifier is adjusted for a maximum output voltage of about 7 V, and its linearity and gain are shown in Fig. 3. The variation of the instantaneous conversion gain over the entire dynamic range is less than 0.5%. This variation includes nonlinearities in a precision mercury pulser² and in a discriminator designed for use with this instrumentation system.

A photograph of an amplifier constructed for laboratory use is shown in Fig. 4. Because capacitive coupling of the output signal to the input reduces the gain, the input stage is isolated from the remainder of the amplifier by a metal shield. Since any pickup of externally generated signals increases the noise, the amplifier is enclosed in a metal box, and the power supplies are decoupled with 1-ms time constants. If possible, the detector should be connected directly to the amplifier in order to avoid the noise and capacity produced by an input cable.

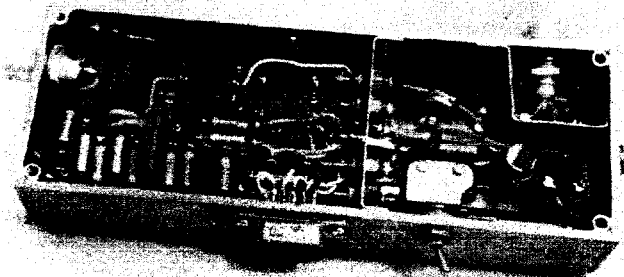


Fig. 4. Laboratory amplifier

Because improper coupling of ground currents can lead to ringing and gain drifts, common ground points, represented by circled numbers in Fig. 2, are used to isolate one stage from another. The metal shield provides a low impedance return for interstage and feedback ground currents.

Capacitive coupling of the base of Q_2 to the collector of Q_3 constitutes positive feedback. In order to avoid the resultant ringing and gain drifts, the base lead of Q_2 on the output side of the shield is kept as short as possible, and the case of Q_2 and Q_3 is grounded. Also, the components in the collector circuit of Q_3 and those associated with Q_1 are kept physically removed from the base of Q_2 . With the above precautions, the effects of pick-up, stray capacity, and ground currents become unobservable.

The amplifier is protected against damage from power supply transients by 100-ohm series decoupling resistors, which limit the current, and by diodes, which prevent breakdown of the relatively delicate emitter-base junctions. The diode on Q_1 also allows current from Q_3 to pull capacitive loads negative, so that even for loads greater than 200 pF, the output pulse shape remains constant.

²RIDL Model 47-7.

V. STABILITY AGAINST OSCILLATION

Because more than two poles are within the feedback loop, oscillation, which would render the amplifier useless, is possible. Because a low gain drift and a large margin of safety against oscillation are competing requirements, the conditions for oscillation were calculated in detail.

Oscillation is possible if 180 deg of phase shift occurs at frequencies less than that frequency for which the absolute value of the feedback factor equals 1 (gain crossover). This phase shift is critically dependent on the detector capacity. In order to prevent oscillation for detector capacities less than 130 pF, the high-frequency gain of the first stage is decreased without increasing amplifier noise by adding a compensating network (R_{c1} and C_{c1}) to the drain of Q_1 . Not only does this network decrease the high-frequency gain, it also produces a zero near gain crossover, resulting in improved phase margin.

Another such zero is provided by a resistor (R_{c3}) in series with the detector capacity. For detector capacities 50 pF or greater, R_{c3} is chosen so that τ_{c3} is fixed at 10 ns. Because a pole tends to cancel the beneficial effect of τ_{c3} for detector capacities much below 50 pF, and because the noise from resistors larger than about 200 ohms becomes significant, R_{c3} is fixed at 200 ohms for detector capacities below 50 pF. The detector bulk resistance also adds to R_{c3} , improving the stability of the amplifier.

The value of C_{c1} is then determined by requiring an adequate gain margin under the worst conditions. Calculation shows that the gain margin at -50°C can be up

to a factor of 2 less than at $+50^\circ\text{C}$. For space applications, C_{c1} is chosen so that the feedback factor for a phase shift of 180 deg at $+50^\circ\text{C}$ is 0.25, leaving an additional factor of 2 at -50°C for transistor variations. Figure 5 shows the resulting values of C_{c1} , R_{c1} , and R_{c3} vs detector capacity.

In the laboratory amplifier, R_{c3} is fixed at 100Ω , and C_{c1} , which can be removed by a switch, has a value of 200 pF. This compensation provides only marginal stability at -50°C for detector capacities less than 25 pF, but even for zero detector capacity oscillation does not occur at room temperature. Reduced gain drift will result if the compensation is switched out for detector capacities exceeding about 70 pF. However, oscillation may occur for detector capacities less than about 50 pF unless the compensation is switched in.

The output compensation, consisting of R_{c2} and C_{c2} (Fig. 2), reduces the sensitivity of the circuit to capacitive loads. Without this compensation, such loads would produce a pole in the complex feedback factor near gain crossover. The output compensation reduces the amplitude of the feedback factor near gain crossover without adding appreciably to the phase shift or to the gain drifts. The pole proportional to the load capacity is then displaced to frequencies considerably higher than the frequency at gain crossover.

Because the prediction of the condition for oscillation is critical in the choice of the compensating elements, the calculated oscillatory conditions were checked experi-

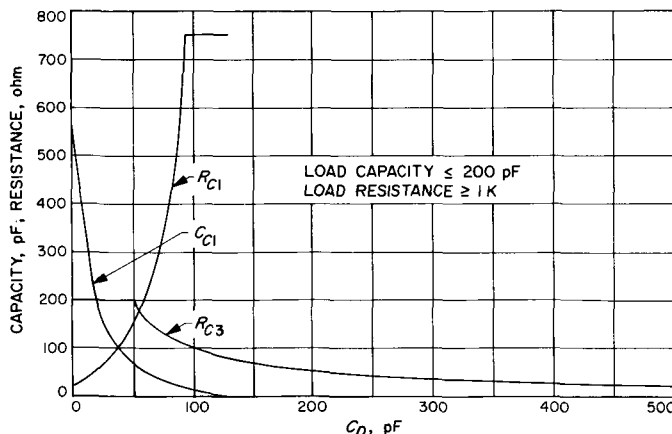


Fig. 5. Compensation values vs detector capacity

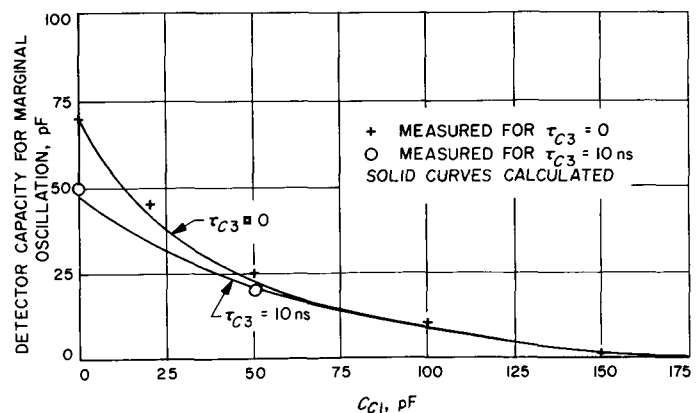


Fig. 6. Conditions for oscillation

mentally. Because frequencies over 10 Mc were involved, a direct measurement of the feedback factor vs frequency was not practical. However, for a fixed compensation scheme, the minimum value of the detector capacity to

prevent oscillation could both be predicted and measured. Figure 6 presents a comparison of these values which provide confidence that amplifier performance was correctly calculated.

VI. GAIN DRIFTS

In order to make use of the inherent $\pm 1\%$ stability of solid state detectors, the amplifier gain drift should not exceed $\pm 1\%$. Because many factors may cause gain shifts of the order of 1% over a 100°C temperature range, an analytical approach was first used to estimate the sensitivity of the gain to various drift-producing factors. Proper choice of components for the critical gain-determining elements was then made, and assurance was obtained that the gain did not depend critically on transistor parameters. Approximate agreement between theoretical predictions and experimental results provided confidence that the measurements were correct and not a special case.

The conversion gain can be written as

$$M_c = \frac{Q_D A_0}{e C_{f1}} \left\{ 1 + E + \frac{\delta A_0}{2A_0} - \frac{\delta A_1}{2A_1} - 0.0766 - 0.144 \left(\frac{\delta \tau_{f1}}{23.3 \mu\text{s}} \right) \right\} \quad (5)$$

where

E = transistor parameter dependent gain correction

$$A_0 = \frac{R_{f2}}{R_{f3}}$$

$$A_1 = \frac{C_{f2}}{C_{f3}} = \frac{1}{A_0}$$

δA_0 = variation of A_0 from its nominal value

δA_1 = variation of A_1 from its nominal value

$\delta \tau_{f1}$ = deviation of τ_{f1} from $23.3 \mu\text{s}$

$$R_{f2} \gg R_{f3}$$

The gain correction dependent on transistor parameters (E) was measured at room temperature as a function of detector capacity and is shown in Fig. 7. Measured and theoretical values agree to within about $\pm 0.7\%$ for detector capacities up to 350 pF.

Metal film resistors with temperature coefficients less than $\pm 25 \text{ ppM}/^\circ\text{C}$ are used for R_{f2} and R_{f3} . The maximum gain drift caused by drifts of these resistors is then less than $\pm 0.13\%$ for a $\pm 50^\circ\text{C}$ temperature change, with partial temperature tracking of the resistors reducing the drift below this value. Similarly, a metal film resistor is used for R_{f1} , even though such a resistor is physically much larger than a composition carbon resistor. However, a carbon resistor could produce a $\pm 7.5\%$ drift in τ_{f1} , resulting in a $\pm 1.1\%$ gain variation over the temperature range. With a metal film resistor for R_{f1} and a glass capacitor for C_{f1} , the drift in τ_{f1} is about $\pm 0.8\%$ over the temperature range, resulting in a gain change of less than $\pm 0.12\%$.

The gain is inversely proportional to C_{f1} , which is provided by a 4.7-pF glass capacitor in parallel with the 0.4-pF capacity associated with R_{f1} . The glass capacitor temperature coefficient, which is specified by the manufacturer³ to be fixed within $\pm 5 \text{ ppM}/^\circ\text{C}$, has a value of about $120 \text{ ppM}/^\circ\text{C}$. A sensistor in series with R_{f2} compensates for the resulting $\pm 0.6\%$ drift in C_{f1} over the temperature range. The drift produced by lack of perfect tracking of the sensistor and the capacitor and by uncertainties in their temperature coefficients is of the order of $\pm 0.2\%$. Because glass capacitors are also used for C_{f2} and C_{f3} , $\delta A_1/2A_1$ is less than $\pm 0.03\%$ over the temperature range.

³Corning Glass Works, Bradford, Pa.

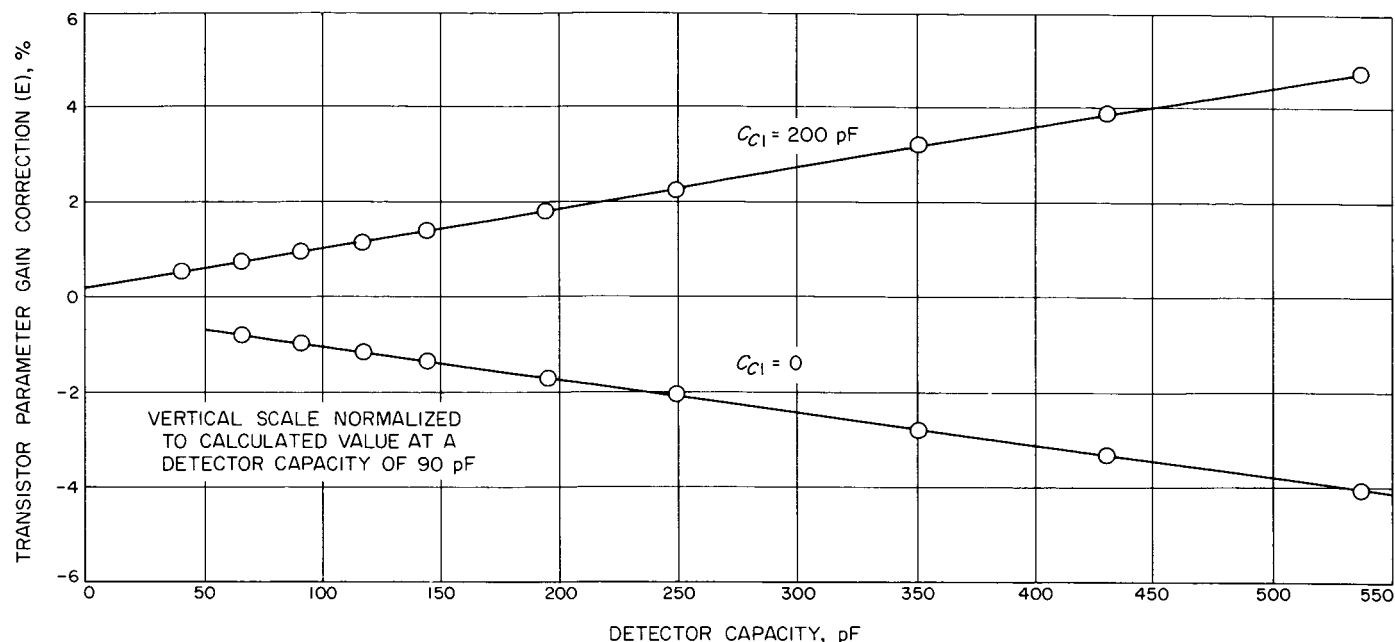


Fig. 7. Gain correction vs detector capacity

Figure 8 shows the measured gain drift with four values of detector capacity for temperatures between -60 and $+100^{\circ}\text{C}$. In almost all cases the calculated drifts agreed with the measured drifts within the uncertainties of the temperature coefficients of the gain-determining resistors and capacitors. The gain drifts for temperatures between -50 and $+50^{\circ}\text{C}$ are less than $\pm 0.5\%$ for detector capacities below 350 pF and less than $\pm 1.0\%$ for detector capacities below 540 pF. Holding the amplifier at 145°C for 24 hr with the power off causes gain changes less than $\pm 0.1\%$.

The output resistance was measured at room temperature by loading the amplifier with a 1K resistor, and observing the difference in output amplitude compared to the unloaded case. The measured output resistance is less than 6 ohms for detector capacities up to 350 pF. Loading the amplifier by 1K adds less than $\pm 0.1\%$ to the gain drifts for temperatures between -50 and $+50^{\circ}\text{C}$

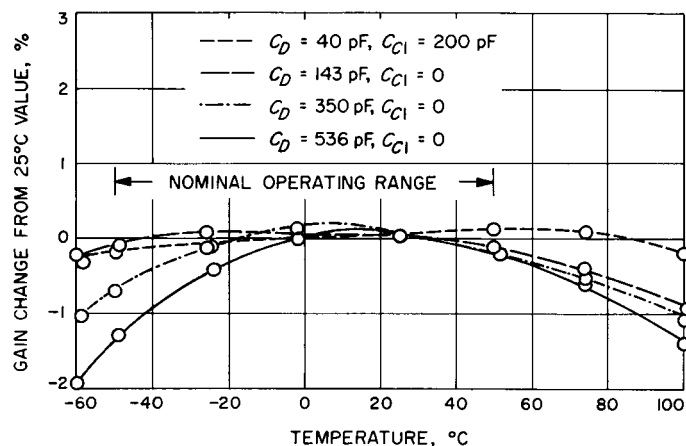


Fig. 8. Gain vs temperature

for detector capacities less than 350 pF, and less than $\pm 0.2\%$ for detector capacities less than 540 pF.

VII. RESOLUTION

Because of the large number of carriers produced by most charged particles entering a detector, the energy resolution of an amplifier-detector system is principally limited by electrical noise (Ref. 3). The dependence of this noise on amplifier parameters is summarized in Table 1. The full width at half maximum counting rate (FWHM) is given by

$$FWHM = 2.35(\overline{E_{nd}^2} + \overline{E_{ng}^2} + \overline{E_{nr}^2} + \overline{E_{nc}^2} + \overline{E_{nl}^2} + \overline{E_{nq}^2} + \overline{E_{nu}^2})^{1/2} \quad (6)$$

where formulas for the individual noise sources are given in Table 1.

The equivalent squared input noise voltage ($\overline{e_n^2}$) was measured for 25 field-effect transistors, and its distribution at room temperature is shown in Fig. 9. As would be

expected (Ref. 4), units exhibiting a large g_m also appear to be the most quiet. However, even among the high g_m units, the equivalent noise voltage varies 2 to 1. From 25 transistors, six satisfy the current and transconductance requirements for laboratory use and are low noise units

$$(\overline{e_n^2})^{1/2} \leq 5.0 \times 10^{-9} \text{ V (cps)}^{-1/2}$$

A unit with an equivalent noise voltage of $4.15 \times 10^{-9} \text{ V (cps)}^{-1/2}$ was used in an amplifier constructed to test the noise theory. Figure 10 shows the calculated and measured noise vs detector capacity. Figure 10 also shows the calculated total energy resolution assuming a 25 keV (FWHM) resolution for the detector. This resolution was checked directly using an Am^{241} source, and the resulting peaks for two detectors with resolution specified to be

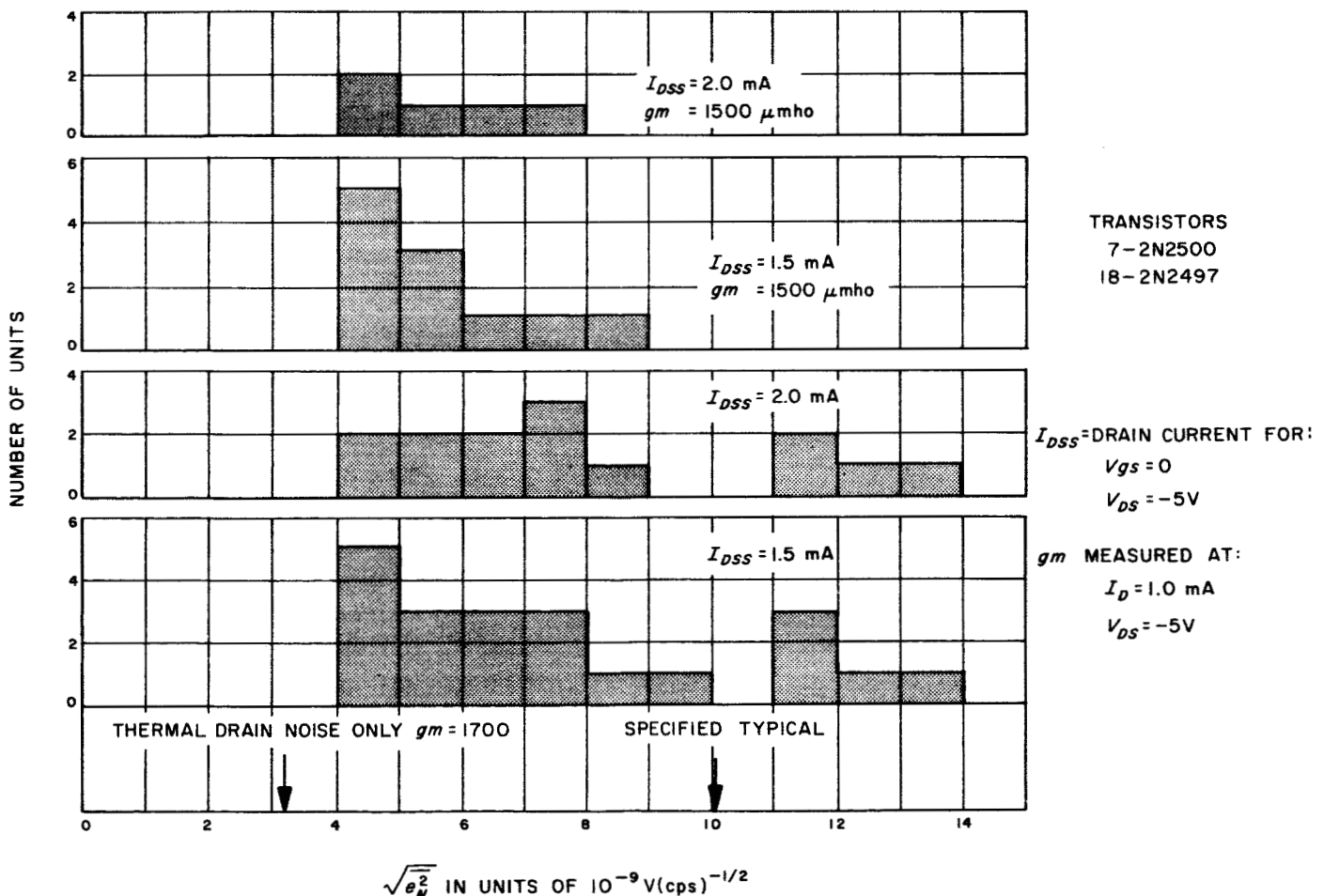


Fig. 9. Distributions of noise voltage for field-effect transistors

Table 1. Formulas for noise sources

Source	Equivalent squared rms noise energy	Source	Equivalent squared rms noise energy
Thermal FET drain noise	$\overline{E_{nd}^2} = \frac{\overline{e_n^2} (C_D + C_B)^2 \left(\frac{eE_0}{q} \right)^2}{8\tau}$ $= \frac{4.54 \times 10^{32} \overline{e_n^2} (C_D + 15 \times 10^{-12})^2}{\tau}$	Thermal noise from R_{cs}	$\overline{E_{nc}^2} = \frac{4kT\tau_{cs}C_D}{8\tau} \left(\frac{eE_0}{q} \right)^2 = \frac{7.14 \times 10^4 C_D}{\tau}$
Gate leakage current noise	$\overline{E_{ng}^2} = \frac{\overline{i_n^2} \tau}{8} \left(\frac{eE_0}{q} \right)^2 = (4.46 \times 10^{32}) \overline{i_n^2} \tau$	Detector leakage current noise	$\overline{E_{nl}^2} = \frac{I_L \tau (eE_0)^2}{4q} = (1.43 \times 10^{14}) I_L \tau$
Detector and FET bias resistor thermal noise	$\overline{E_{nr}^2} = \frac{4kT\tau}{R_D 8} \left(\frac{eE_0}{q} \right)^2 = (1.76 \times 10^6) \tau$	Statistical variation in the number of carriers produced	$\overline{E_{nq}^2} = EE_0$
		Variations in collection efficiency	$\overline{E_{nv}^2} = \text{depends on construction of detector}$
Equivalent squared noise energy in (keV) ² E_0 = energy per hole-electron pair = 3.5 eV in silicon C_B = amplifier input capacity for the drain of Q_1 grounded = 15 pF C_D = detector capacity, F $\overline{e_n^2}$ = equivalent squared input noise voltage of FET $\overline{i_n^2}$ = equivalent squared input noise current of FET		R_D = parallel value of detector bias resistor and FET bias resistor I_L = detector leakage current $\tau_{cs} = R_{cs}C_D$ T = absolute temperature = 298°K τ = shaping time constant, sec	

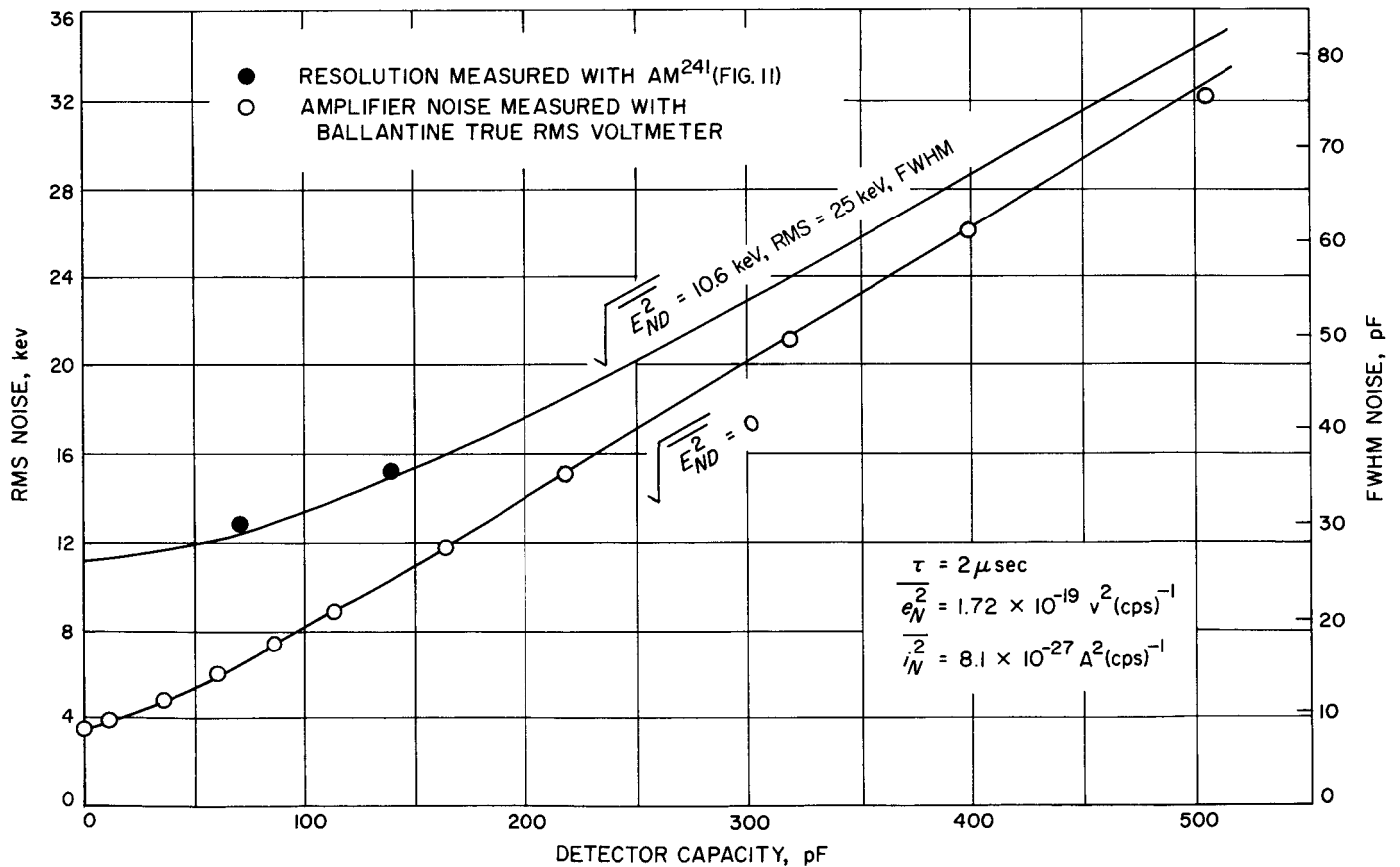


Fig. 10. Equivalent input noise energy

25 keV are shown in Fig. 11. Because of the low-energy tail caused by emission to excited states and by scattering, the resolution was calculated by doubling the upper half width at half maximum. The amplifier gain, which was measured to be 0.98 V/MeV, is within the tolerances of the gain-determining elements. The calculated and measured resolutions are compared in Fig. 10.

For applications where resolution is most critical, further optimization is possible by varying the shaping time constant. The total resolution may be expressed as

$$\overline{E_{nt}^2} = \overline{E_{nq}^2} + \overline{E_{nu}^2} + \frac{D}{\tau} + E\tau \quad (7)$$

where

$$D = (7.73 \times 10^{-3})(C_D + 15)^2 + 7.14 \times 10^{-2}C_D \quad (\text{keV})^2 (\mu\text{s})$$

$$E = 143I_L + 5.38 \quad (\text{keV})^2 (\mu\text{s})^{-1}$$

C_D = detector capacity, pF

I_L = detector leakage current, μA

τ = clipping and integrating time constants, μs

The best resolution results when the shaping time constant is

$$\tau_{opt} = \left(\frac{D}{E}\right)^{\frac{1}{2}} \quad (8)$$

and has a value given by

$$\overline{E_{opt}^2} = \overline{E_{nq}^2} + \overline{E_{nu}^2} + 2(DE)^{\frac{1}{2}}$$

In Fig. 12, τ_{opt} and $(\overline{E_{opt}^2})^{\frac{1}{2}}$ are plotted vs detector capacity for a leakage current of 0.1 μA . The resolution for a constant 2- μs shaping time constant is shown for comparison.

Naturally, if the shaping time constant is varied, the high-frequency compensation will have to be changed

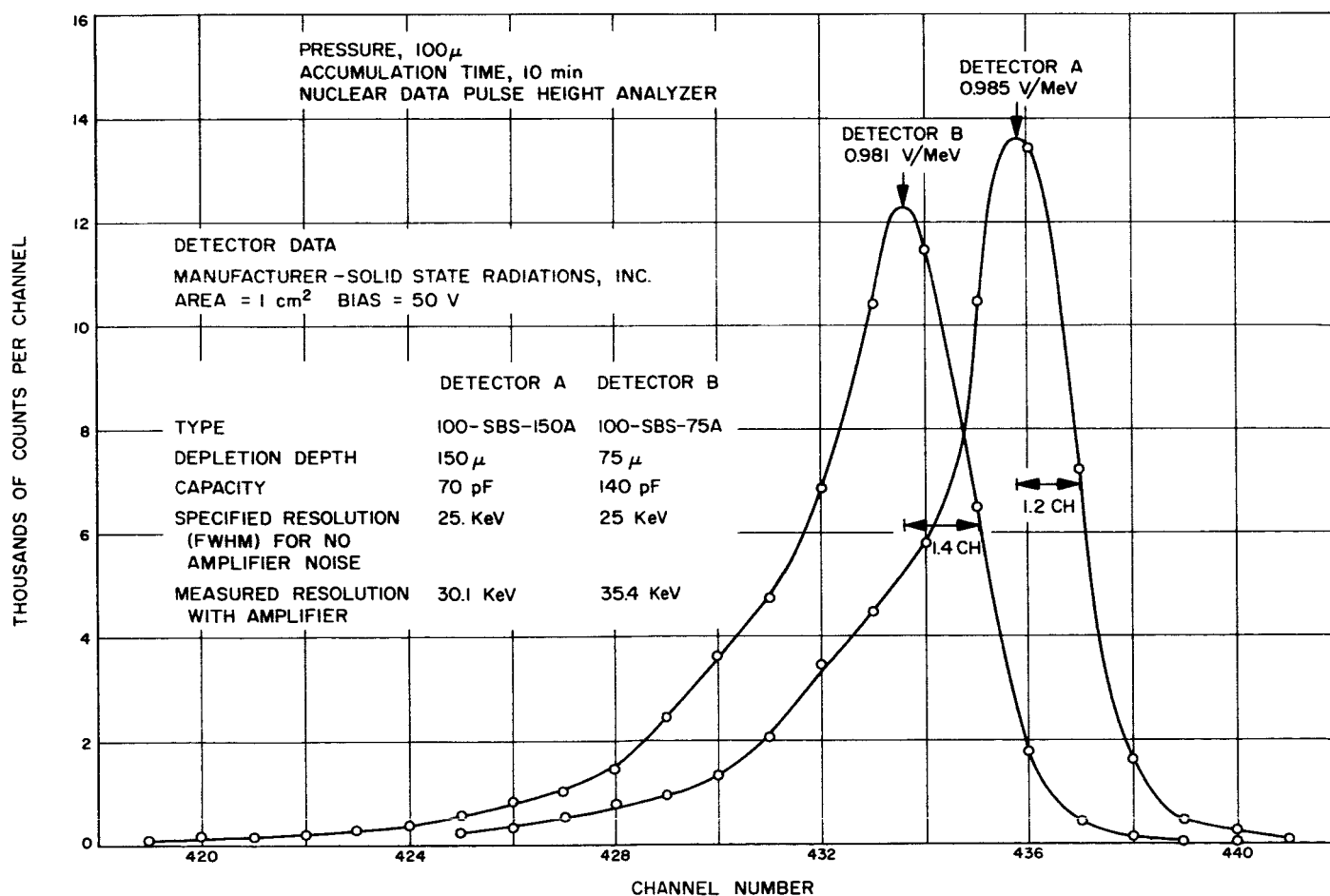


Fig. 11. Spectra of Am^{241}

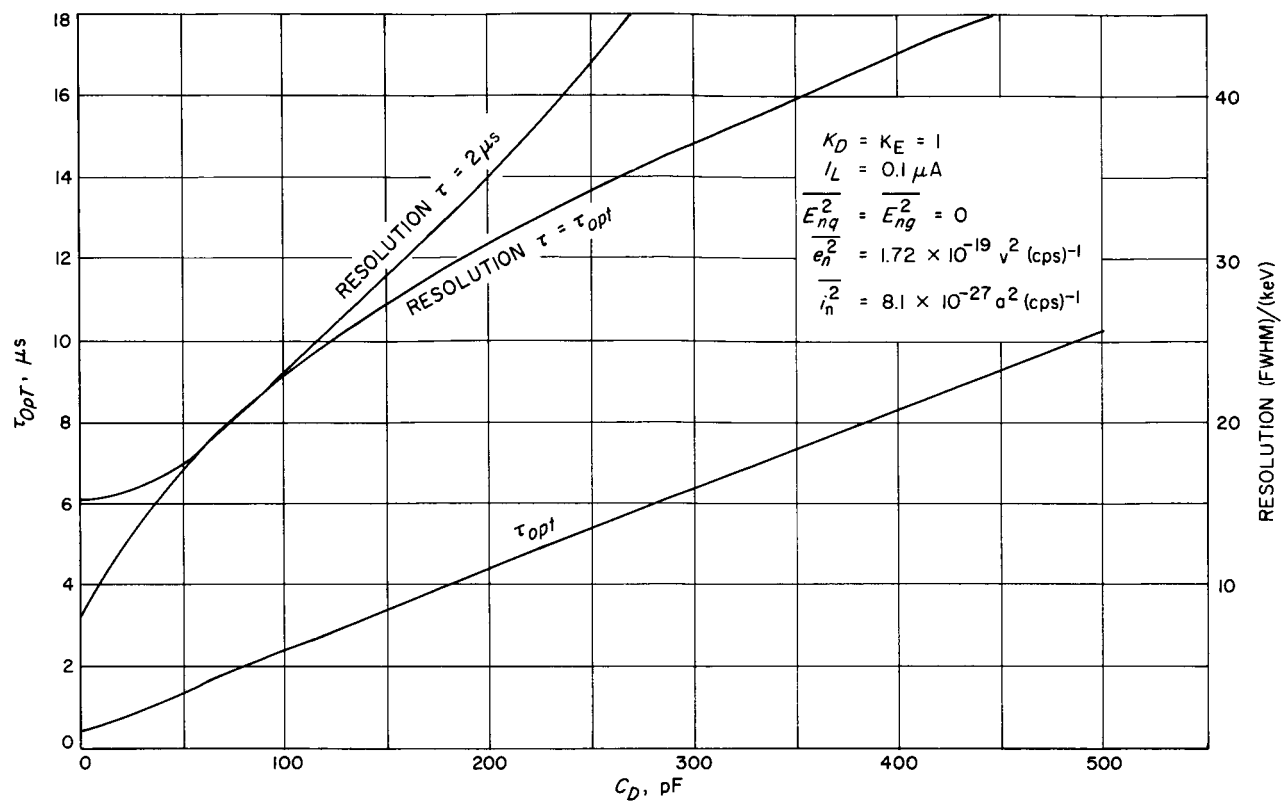


Fig. 12. Optimum shaping time constant and resolution

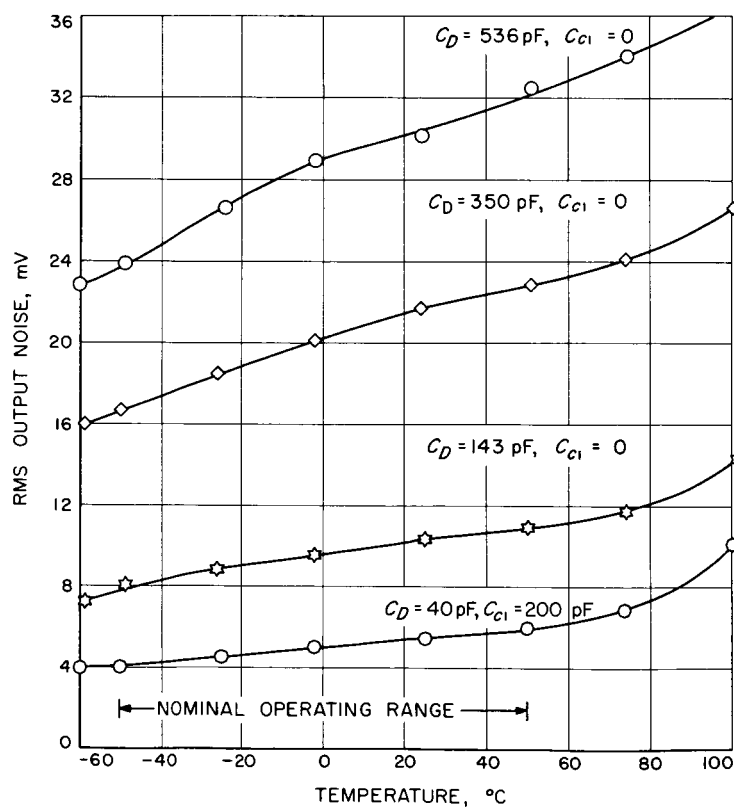


Fig. 13. Noise vs temperature

accordingly. If the shaping time constant becomes too short, excessive gain drifts may result. Conversely, long shaping time constants may cause difficulty with tail pile-up at high repetition rates.

Figure 13 illustrates the dependence of amplifier noise on temperature. For temperatures below about 70°C,

field-effect transistor channel noise dominates, and the noise is roughly proportional to the absolute temperature. Above 70°C, gate leakage current, which rises exponentially with temperature, becomes significant. For detectors having leakage currents of about 0.1 μA at room temperature, the exponential rise of noise with temperature would probably begin near 50°C.

REFERENCES

1. Franzgrote, E., and Marshall, J. H., "Analysis of the Martian Atmosphere by Alpha Particle Bombardment," SPS 37-26, Vol. 4, Jet Propulsion Laboratory, Pasadena, Calif.
2. Fairstein, E., "Considerations in the Design of Pulse Amplifiers for Use with Solid State Radiation Detectors," Tennelec Instrument Co., Oak Ridge, Tenn.
3. Taylor, M. M., *Semiconductor Particle Detectors*, Butterworths, London.
4. Van der Ziel, A., "Thermal Noise in Field-Effect Transistors," *Proc. IRE*, Vol. 50, August 1962, pp. 1808-1812.